Chaotic and regular behavior in two-dimensional anharmonic crystal lattices

M. L. A. Nip, J. A. Tuszyński, Z. W. Gortel, and T. A. Riauka
Department of Physics, University of Alberta, Edmonton, Alberta, Canada T6G 2J1
(Received 30 June 1992; revised manuscript received 10 May 1993)

A two-dimensional anharmonic lattice model to describe the behavior of coupled nonlinear displacement modes is constructed. The equations of motion and the underlying Hamiltonian of the anharmonic lattice are found. The equations of motion are analyzed using the fourth-order Runge-Kutta method. The integrability of the system is found to depend on its energy as well as the regularity of the system potential. A continuous transition between regular and chaotic behavior is found and is illustrated using Poincaré sections. As an example, the effects of ordering on a (100) tungsten surface are discussed in this context.

I. INTRODUCTION

A large variety of condensed matter systems exhibit properties which manifest underlying competition between two distinct types of order. Examples of such behavior include metamagnets,[1] ferroelectric-ferromagnetic systems,[2] ferroelectric-piezoelectric crystals,[3] and crystalline-superfluid systems[4] as well as orientation-position ordering phenomena in molecular liquid crystals.[4] It is well known that an interplay between two distinct orders may result in critical temperature shifts as well as crossover phenomena. This can be readily analyzed using the mean-field approximation.[5] However, a more fundamental microscopic approach to the problem poses a serious difficulty due to inherent nonlinearities in the description.

Denoting the order parameters corresponding to the two coupled subsystems by q_1 and q_2 and their conjugate momenta by p_1 and p_2, respectively, the following quartic Hamiltonian has been a frequent choice for the semiclassical modeling of this type of problem:

$$H = \frac{1}{2}(p_1^2 + p_2^2) + \omega_1 q_1^2 + \omega_2 q_2^2 + \beta q_1^2 q_2^2 + \alpha(q_1^4 + q_2^4). \tag{1.1}$$

This type of Hamiltonian has been used in the context of ferroelectric-ferromagnetic,[2] ferroelectric-piezoelectric,[6] and commensurate-incommensurate transitions in crystals,[7] and several types of smectic liquid crystal transformations[8,9] to name but a few of its useful applications. The same Hamiltonian arises also in an extension of the continuum approximation to the one-dimensional Hubbard model of the metal-insulator transition.[10]

A separate class of applications of the class of Hamiltonians exemplified by Eq. (1.1) has emerged in studies of two-dimensional nonlinear lattices.[11–15] It is on this latter context that this paper will be focused. The primary interest will be directed towards elucidating the question of regular versus chaotic behavior in two-dimensional monatomic crystal lattices. While periodic orbits can be regarded as classical analogs of anharmonic phonon modes, chaotic behavior may be indicative of disorder and even melting effects.

II. THE MODEL

A two-dimensional monatomic crystal lattice, as shown in Fig. 1, is considered. Each lattice site is occupied by a single atom and each atom is coupled to its four nearest neighbors by harmonic "springs" (elastic forces). To make the model more general, the lattice is allowed to be characterized by two inequivalent lattice constants a and b so that the basic unit cell of the lattice need not be a perfect square. As a result, anisotropy is directly built into the model. Thus, the total potential energy of the lattice has two components: One component is due to the isotropic atomic interactions and the other component represents the anisotropy energy. The latter is responsible for any deviations from the square symmetry. However, in order to reduce the complexity of the computation, the anisotropy energy is removed and only rectangular lattices are considered. Consequently,

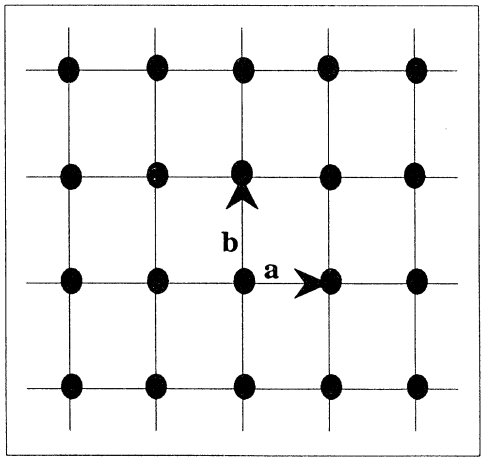

FIG. 1. A two-dimensional monatomic rectangular lattice with two lattice constants a and b.

 ©1993 The American Physical Society

the potential energy of the system is constructed entirely from two-body central potentials. Since the lattice consists of one kind of atom, only one type of two-body potential is involved in the calculations.

It is not difficult to demonstrate that the following generic Lagrangian density has all the required features to properly describe the crystal lattice under consideration:

$$\mathcal{L}=\sum_{i=1}^{2}\left\{\frac{m}{2}\left(\frac{\partial u_i}{\partial t}\right)^2-\frac{\sigma_{ii}}{2}\left(\frac{\partial u_i}{\partial x}\right)^2-\frac{\zeta_{ii}}{2}\left(\frac{\partial u_i}{\partial y}\right)^2 -\frac{S_{ii}}{2}u_i^2-\frac{L_{iiii}}{4}u_i^4\right\}-\frac{3}{2}\lambda u_1^2u_2^2\ , \tag{2.1}$$

where u_1 and u_2 are the two orthogonal lattice displacement fields, m is the mass of a single lattice site, and the coefficients in Eq. (2.1) are all assumed to be model-dependent constants. Then, under Legendre transformation, the corresponding Hamiltonian density is given by

$$\mathcal{H}'=\sum_{i=1}^{2}\left\{\frac{m}{2}\left(\frac{\partial u_i}{\partial t}\right)^2+\frac{\sigma_{ii}}{2}\left(\frac{\partial u_i}{\partial x}\right)^2+\frac{\zeta_{ii}}{2}\left(\frac{\partial u_i}{\partial y}\right)^2 +\frac{S_{ii}}{2}u_i^2+\frac{L_{iiii}}{4}u_i^4\right\}+\frac{3}{2}\lambda u_1^2u_2^2. \tag{2.2}$$

Using Euler-Lagrange equations, it is easy to show that the equations of motion for the two displacement fields take the form

$$m\frac{\partial^2 u_\rho(\mathbf{r})}{\partial t^2}=\sigma_{\rho\rho}\frac{\partial^2 u_\rho}{\partial x^2}+\zeta_{\rho\rho}\frac{\partial^2 u_\rho}{\partial y^2}-S_{\rho\rho}u_\rho -L_{\rho\rho\rho\rho}u_\rho^3-3\lambda u_\rho u_\alpha^2\ . \tag{2.3}$$

The wave equation (2.3) is a partial differential equation in both space and time. This equation calls for a finite-difference algorithm and can be solved with appropriate boundary conditions. As a special case, we shall assume traveling-wave solutions of the form

$$u_\rho=u_\rho(\mathbf{k}\cdot\mathbf{r}-\omega t)=u_\rho(z) \tag{2.4}$$

and reduce Eq. (2.3) to an ordinary differential equation. For both numerical convenience and physical insight, three dimensionless variables X, Y, and T are introduced and the dependent and independent variables are scaled according to

$$z=\tau T,\quad u_1=\mu X,\quad u_2=\nu Y. \tag{2.5}$$

This transforms the wave equation (2.3) into two dimensionless component equations of motion on X and Y as

$$\frac{d^2X}{dT^2}=K_XX-X^3+DXY^2 \tag{2.6}$$

and

$$\frac{d^2Y}{dT^2}=K_YY-Y^3+DYX^2, \tag{2.7}$$

provided the following relations hold:

$$\begin{aligned}
&\Omega=\sigma_{11}k_x^2+\zeta_{11}k_y^2-m\omega^2\ ,\\
&\Phi=\sigma_{22}k_x^2+\zeta_{22}k_y^2-m\omega^2\ ,\\
&\frac{\tau^2\mu^2L_{1111}}{\Omega}=\frac{\tau^2\nu^2L_{2222}}{\Phi}=-1\ ,\\
&\nu^2\Phi=\mu^2\Omega\ ,\\
&K_X=\frac{\tau^2S_{11}}{\Omega}\ ,\\
&K_Y=\frac{\tau^2S_{22}}{\Phi}\ ,\\
&D=\frac{3\tau^2\mu^2\lambda}{\Phi}=\frac{3\tau^2\nu^2\lambda}{\Omega}.
\end{aligned} \tag{2.8}$$

The equations of motion (2.6) and (2.7) can be looked upon as a system of two coupled anharmonic oscillators vibrating in two orthogonal directions. When the coupling is weak, the two oscillators are essentially independent of each other and the system appears integrable. It is well known that, for an integrable system, there exists an additional conserved quantity besides the energy such that the trajectory for a given energy and initial conditions lies on the surface of an invariant torus so that the system behaves regularly. However, the integrability of the system and the invariant torus can be destroyed by increasing the coupling between the oscillators. This leads to the appearance of chaotic motion. The degree of chaos depends on the amount of perturbation on the integrability of the system. This question will be investigated in considerable detail in the following section. It was first pointed out by Ali and Somorjai[16] that a nonlinear Hamiltonian system regains its integrability at very high energies and this results in the reappearance of regular motion. Therefore, intuitively, our system is expected to behave regularly at low and at very high energies and behave chaotically at intermediate energies. To illustrate these order-disorder transitions, surfaces of section (Poincaré sections) are constructed to examine the evolution of the system in phase space. However, before proceeding further, the system's behavior must be looked at in greater detail. Since the Hamiltonian contains all the dynamical information about the system, it seems logical to obtain an effective Hamiltonian density that corresponds to the reduced equations of motion, Eq. (2.6) and Eq. (2.7). The following dimensionless Hamiltonian density is found:

$$\mathcal{H}=\frac{P_X^2}{2M_X}+\frac{P_Y^2}{2M_Y}-\frac{1}{2}\left(K_XX^2+K_YY^2\right) +\frac{1}{4}\left(X^4+Y^4\right)-\frac{D}{2}X^2Y^2\ , \tag{2.9}$$

where $\mathcal{H}$ is scaled according to $\mathcal{H}'=\varepsilon\mathcal{H}$ and the symbols used have the values

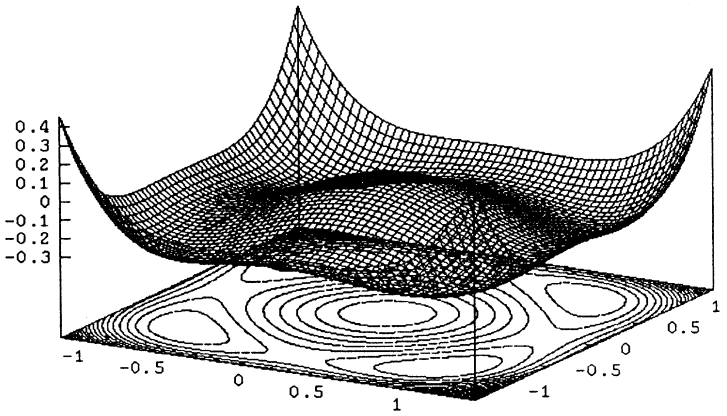

FIG. 2. Contour plot of the system potential.

$$
\begin{aligned}
M_X &= -\left(\frac{2m\omega^2}{\Omega}+1\right) , \\
M_Y &= -\left(\frac{2m\omega^2}{\Phi}+1\right) , \\
P_X &= M_X \frac{dX}{dT} , \\
P_Y &= M_Y \frac{dY}{dT} , \\
\varepsilon &= -\frac{\Omega\mu^2}{\tau^2} .
\end{aligned}
\tag{2.10}
$$

This Hamiltonian density provides sufficient information to acquire an intuitive understanding of the behavior of the system.

A contour plot of the system potential in the Hamiltonian density Eq. (2.9) is displayed in Fig. 2, where $K_X = K_Y = 1$ and $D = -1/2$ have been chosen for simplicity. The potential has a local maximum at the origin of the coordinate system and four local potential wells, one in each quadrant, surrounding the central peak. Furthermore, there is a saddle point halfway between any two neighboring wells. Thus, the system exhibits fourfold symmetry. An interesting property of the potential can be exposed by dissecting the potential surface in two ways. First, the potential surface is dissected with the vertical plane that contains the saddle point on the extreme right of Fig. 2 and is oriented along the x axis. Second, the potential surface is dissected diagonally with the vertical plane that contains the origin and is oriented in the $(1,1)$ direction. In both cases, the intersection of the potential surface with the vertical plane exposes a symmetric double-well shape. These double-well potentials provide an additional explanation for the chaotic motion of the system.

Our system can be regarded as a phonon quasiparticle with two coupled vibrational modes. If the energy of the phonon is sufficiently low, with the appropriate initial conditions, we can place the phonon at the bottom of one of the potential wells. At these energies, the motion of the particle is very restrictive; the value of X is approximately the same as that of Y. As a result, the coupling terms in the equations of motion (2.6) and (2.7) become ineffective. The two oscillators are decoupled; the system exhibits regular motion. But, as soon as we lift the energy of the phonon, its amplitude of oscillation increases correspondingly. The coupling terms in the equations of motion now become highly effective. Chaotic motion appears if the coupling is sufficiently strong. As the energy of the phonon rises above the saddle point but remains below the central peak, the system becomes ever more chaotic. In this regime, the coupling strength between the oscillators reaches its highest value. We can interpret the system's behavior at these energies in a slightly different way. At these energies, two or more potential wells are accessible to the particle; it becomes impossible to predict the particle's trajectory in phase space. In the other extreme, when the energy of the phonon is very high, the particle sees a smooth varying potential and is insensitive to its minute variation near the origin. Also, as pointed out by Ali and Somorjai,[16] the contribution of the coupling terms to the total energy of the system decreases with increasing energy. Thus, in this high-energy regime, the oscillators are once again decoupled and the system regains its regularity. In the next section, we illustrate these qualitative statements with a wealth of data from numerical simulations.

III. OVERVIEW OF NUMERICAL RESULTS

To test our conjectures, we integrated the dimensionless equations of motion (2.6) and (2.7), for $K_X = K_Y = 1$ and $D = -1/2$, using the fourth-order Runge-Kutta method with a step size of 0.0005 to ensure numerical accuracy. We demonstrated the regular and the chaotic motion of the system by the Poincaré surfaces of section, each of which was constructed by plotting the momentum P_Y against Y every time the particle crossed the point $x = \sqrt{\frac{2}{3}}$ with a positive momentum P_X. The investigated energies were -0.33, -0.31, -0.275, -0.2499, -0.24, -0.05, 1, 10, and 1000, but only several representative surfaces of section were reproduced and shown in the figures. At each energy value, at least six different orbits were generated. Each regular orbit was allowed to pierce the surface of section at least 300 times, whereas

each irregular (chaotic) orbit was allowed to pierce the surface at least 500 times.

At the energy of -0.33, the particle is lying very close to the bottom of one of the potential wells. As we have already mentioned, we expect the two oscillators to be decoupled at this energy. For all the initial conditions we put in, the orbits we obtained were all regular. These orbits are shown in Fig. 3. There is no sign of chaos anywhere in the figure. It appears that chaos begins to emerge at the energy of -0.31. As shown in Fig. 4, at this energy, some of the regular orbits bifurcate into two closed loops divided by a separatrix denoted by s in the figure. Although not shown here, chaotic motion can be seen to be confined within the separatrix. We can take this as an indication of which of the coupling terms in the dimensionless equations of motion becomes effective. At the energy of -0.2499, the system's integrability is seriously diminished. All of the potential wells are now accessible to the particle; therefore, as depicted in Fig. 5, the surface of section has expanded to two separate parts. Furthermore, chaotic motion has dominated the picture; the regular structure has begun to disappear. Right below the central peak of the potential, at the energy of -0.05, the regular structure has shrunk to an infinitesimally small region of the surface if it has not vanished completely. All orbits we have generated are chaotic. This surface of section is depicted in Fig. 6. We expect the system to regain its regularity at very high energies. We found that this is indeed correct. As demonstrated in Fig. 7, the regular structure has reappeared and dominated the surface at the energy of 1000.

It is interesting to note that a particular regular orbit called the separatrix can be seen in Figs. 3, 4, 5, and 7 as delineating the regions of local oscillations around a single potential well from large scale oscillations involving several potential wells. In a paper investigating coupled nonlinear wave equations Hawrylak *et al.*[17] reduced their problem to two equations identical in form to our Eqs. (2.6) and (2.7). They found three general types of solutions corresponding to separatrix motion. Type-1 solutions are a topological soliton coupled to a stationary

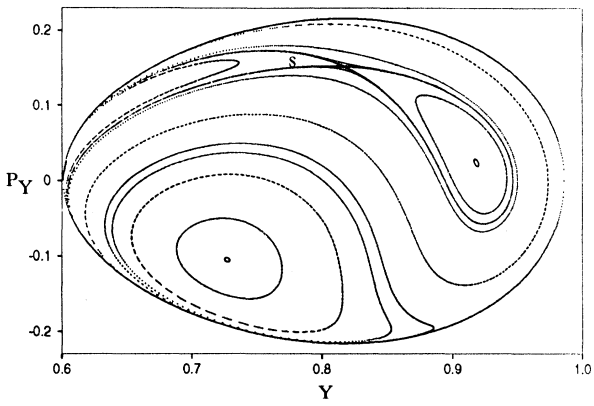

FIG. 4. Poincaré section at the energy of -0.31.

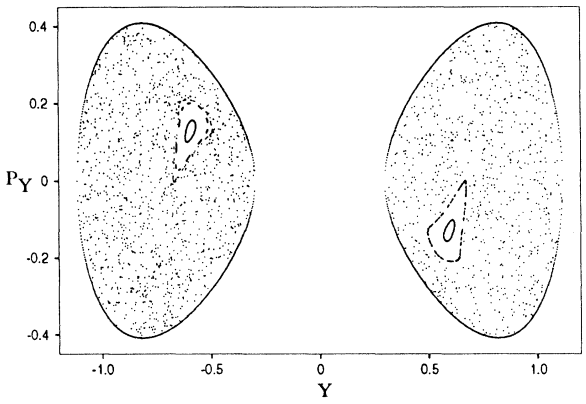

FIG. 5. Poincaré section at the energy of -0.2499.

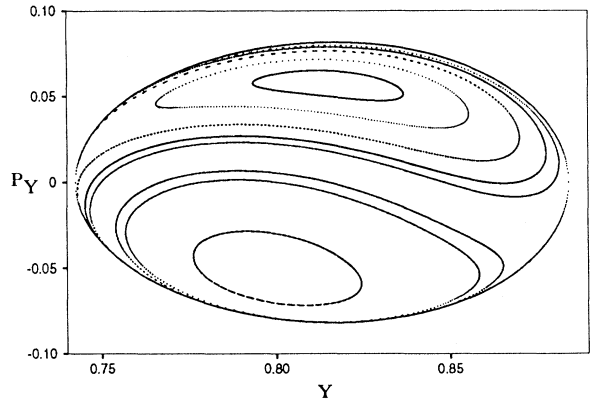

FIG. 3. Poincaré section at the energy of -0.33.

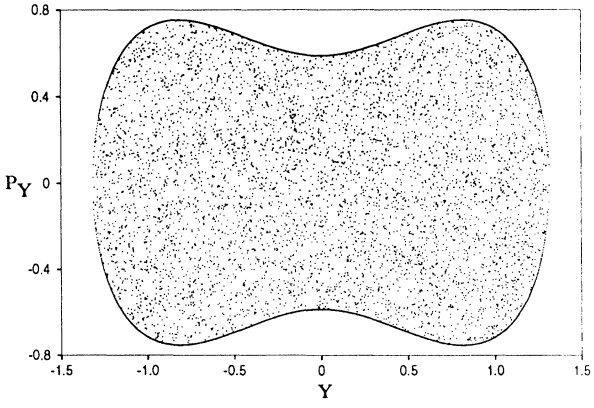

FIG. 6. Poincaré section at the energy of -0.05.

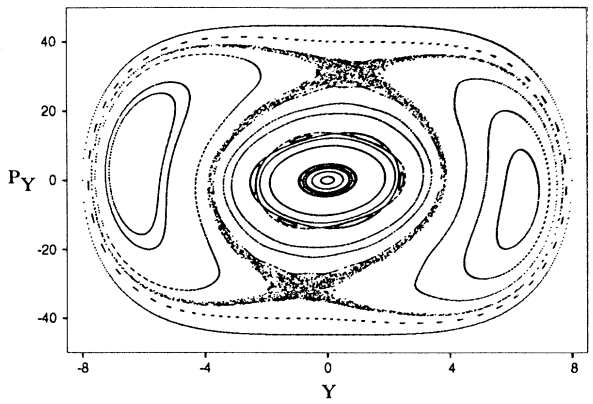

FIG. 7. Poincaré section at the energy of 1000.

solution. Type-2 solutions represent a pair of topological and nontopological solitons (tanh and sech functions of the independent variable). Finally, type-3 solutions (which are unstable) could not be expressed in closed form.

Of particular importance, especially from the point of view of semiclassical quantization, are periodic orbits. They can eventually serve as classical analogs of anharmonic phonons in a lattice. The next section attempts to investigate their role in the dynamics of the two-dimensional lattice considered in this paper.

IV. FINDING PERIODIC ORBITS

In this section, methods are presented for the determination of initial conditions that give rise to periodic orbits at intermediate energies where the motion is predominantly chaotic. At these (intermediate) energies invariant tori are broken but there still exist an infinite number of periodic orbits of zero measure. As mentioned in Sec. III, the Poincaré surface of section provides a simple method to determine the extent of regular and chaotic motion. By examining periodic orbits that lie within regions of phase space dominated by chaotic motion, the finer details (i.e., microscopic details) of the phase space structure can be investigated. There is also much interest in finding periodic orbits because of their importance in semiclassical quantization; see, for example, Refs. 18–22. These periodic orbits are difficult to determine in general but many can be found numerically for a given energy E. Three numerical techniques were investigated in this work to determine the initial conditions that give rise to a periodic orbit.

We look for periodic orbits belonging to either one of the two classes: (i) the ones which strike the potential boundary ($P_X = P_Y = 0$) at right angle or (ii) the ones which, at least once, cross at right angle one of the symmetry axes ($x = 0$ or $y = 0$) of the constant energy contour. The most successful method used can be called the "symmetry-boundary" technique in which a total energy is fixed first and a sample trajectory is evolved from the potential boundary (or from the symmetry axis) until it reaches the boundary (or the axis not necessarily for the first time). Then an angle between the trajectory and the boundary (or the symmetry axis) normal is calculated and the initial conditions are slightly modified until this angle is reduced to zero within the prescribed accuracy. This technique is computationally efficient and solutions are constrained to an energy manifold implicitly by the choice of the initial conditions. This method was used to obtain the bulk of the periodic orbits for this study and a sample set of these orbits is shown in Fig. 8. It should be noted that although this method is intuitively appealing and simple to implement numerically it provides only a subset of all the periodic orbits of Eqs. (2.6) and (2.7) for a given energy.

Two other techniques were also investigated for determining periodic orbits. The first of these methods is really a numerical definition of a periodic orbit. Here, an initial condition is evolved numerically according to Eqs. (2.6) and (2.7) and at each point in the time evolution one checks whether the orbit returns to the initial conditions. This method requires a $2N$-dimensional search of the phase space for which the time variable has no upper bound. Thus, the method is numerically inefficient. The second method investigated provides a more general class of orbits but is much more computationally demanding than the "symmetry-boundary" technique. This method is based on a Fourier decomposition technique.[24,25] Since we are interested in solutions to Eqs. (2.6) and (2.7) that are periodic in time, we expand X and Y as

$$X(t) = \sum_{n=-N/2}^{N/2} A_{1,n} e^{in\nu_r t} , \tag{4.1}$$

$$Y(t) = \sum_{n=-N/2}^{N/2} A_{2,n} e^{in\nu_r t} , \tag{4.2}$$

where ν_r is a commensurable frequency given by $\nu_r = m\nu_1 = n\nu_2$, with m and n being integers and ν_1 and ν_2 being frequencies of the orbits in the respective dimensions (i.e., X and Y dimensions). Substituting Eqs. (4.1) and (4.2) into Eqs. (2.6) and (2.7) gives $2N + 2$ coupled equations for the $2N + 2$ time-independent Fourier coefficients which can be solved numerically using a multidimensional Newton method. If the solution converges, the construction of the solution guarantees that it is periodic in time. This method has shown to be successful for third-order potentials such as the Henon-Heiles potential,[24] but for our quartic potential this technique becomes too computer demanding to be effectively employed. Periodic orbits were obtained at various energies

but convergence was slow and heavily dependent upon the damping factor for Newton's method.

We note finally that after obtaining many periodic orbits of different periods for a given energy E (see Fig. 8), the classical action and Liapunov exponents were calculated for each. Further, the periodic orbits were either classified as adiabatically stable (attractor) or adiabatically unstable (repellors).[23] It has been conjectured—and we have reason to believe from our own study that this is true—that periodic orbits that are adiabatically stable and have small actions possess particularly interesting properties from the point of semiclassical quantization for which they were successfully used.[23,24]

In the following section we briefly present a physical example with which the model outlined in this paper shows qualitative similarities.

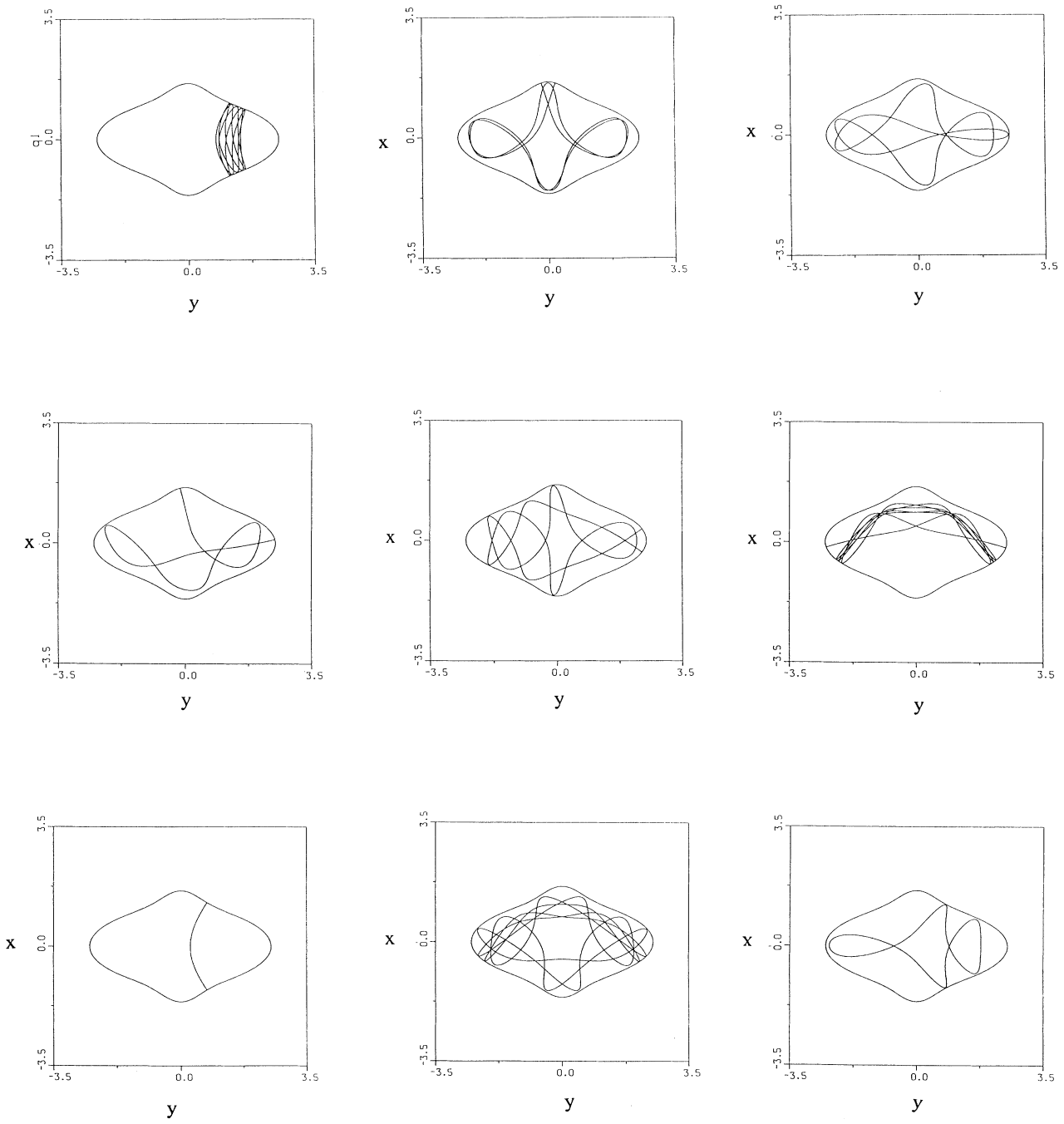

FIG. 8. A selection of nine periodic orbits determined by the symmetry-boundary method for $E = 0.21$.

V. A PHYSICAL EXAMPLE

The results obtained using the low-energy electron diffraction (LEED) technique demonstrated the existence of a second-order structural phase transition on a crystal lattice plane along the (100) direction in the tungsten (W) system at a temperature about 300 K.[26] At the same time, a similar behavior was also observed on the molybdenum (100) surface. These findings lead to the conclusion that the basic mechanism responsible for the transition is likely to be the same for both surfaces. Furthermore, there is clear evidence from LEED that the transition is confined to the top layer of the lattice planes.[27,28] Since the interlayer couplings do not play a significant role in the transition, the phase transition is considered to be two dimensional. Since tungsten has a bcc lattice structure, its lattice planes in the (100) direction are simply two-dimensional square lattices. In principle, we can construct a two-dimensional lattice model to describe the structural change observed provided the model is sufficiently anharmonic, since anharmonicity is an essential ingredient in the phenomenological description of structural phase transitions.

Early theoretical studies on tungsten surface reconstruction suggest that its low-temperature phase corresponds to small oscillations with respect to the displaced potential minima while its high-temperature phase corresponds to large-amplitude oscillations due to the anharmonicity of the effective potential.[29] Consequently, the transition seems to be driven by the softening of the surface-phonon mode. The nature of the transition is further clarified by a recent investigation of the tungsten surface reconstruction by means of Monte Carlo simulations.[30] This latter investigation shows that the transition is of order-disorder type (continuous) and takes place at $T_c = 240$ K. At the transition temperature the pattern of displacements from the equilibrium positions becomes random as shown in Fig. 9.

We believe that the theoretical model discussed in this paper can provide an adequate phenomenological description of the structural phase transition of a tungsten (100) surface. In this respect, we can regard the low-energy regular phase of the lattice (depicted in Fig. 1) as the low-temperature phase of the tungsten surface, whereas the relatively high-energy chaotic phase of the lattice (shown in Fig. 6) can be taken as the high-temperature phase of the tungsten surface. This identification is to be understood in the statistical sense where the mean energy $\langle E \rangle$ of the system is a function of temperature and, in particular, for low temperatures where the system is only weakly anharmonic $\langle E \rangle \approx k_B T$ with k_B denoting the Boltzmann constant. Obviously, at higher temperatures this type of relationship becomes nonlinear. Temperatures corresponding to the energy levels close to the separatrix will cause a severe destabilization of the lattice dynamics leading to a disordered phase. This result agrees qualitatively well with the Monte Carlo simulations carried out recently by Han and Ying[30] for the tungsten surface. They have shown that the low-temperature phase of the tungsten surface corresponds to an orderly oriented displacement phonon field while its high-temperature phase corresponds to a randomly oriented one. In addition, since our solutions to the equations of motion represent the displacement phonon field, our results, consistent with an early investigation,[29] also indicate that the low-temperature phase corresponds to small-amplitude oscillations about the potential minima and that the transition is driven by the softening of the surface-phonon mode. Our model, however, is somewhat more general since it predicts the existence of an additional regular phase beyond the chaotic phase. That this phase does not appear to be physically realized by the tungsten surface does not necessarily invalidate the model itself. In this connection, it must be realized that the equations of motion derived for a perfectly periodic lattice cannot be readily extended beyond the energies corresponding to chaotic (separatrix) motion. At this critical energy level the lattice structure has been virtually destroyed and the validity of the continuum approximation used to derive the equations is no longer present. As a result, a disordered state has set in with a completely irregular positional structure. It is perhaps worth noting that surface reconstruction

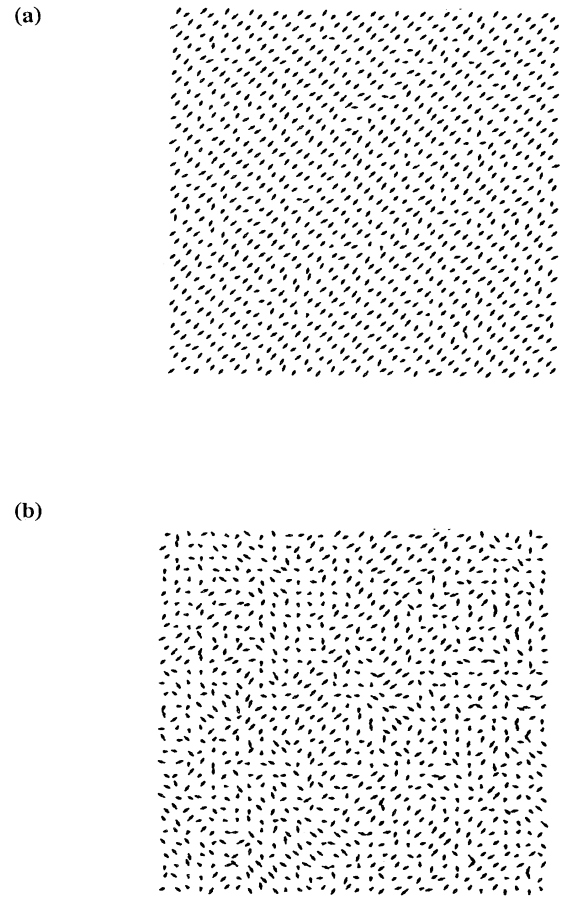

FIG. 9. The snapshots of displacement patterns for tungsten at (a) $T = 110$ K and (b) $T = 240$ K, following Ref. 30.

has also been found to take place on the Si(111), the Ge(111), and the Ge-Sn(111) lattice planes which have a honeycomb structure.[31] Although our results are not directly applicable to these systems, by adopting a triangular underlying lattice and carrying out the similar steps as outlined in the sections above, we can obtain an analogous set of nonlinear equations of motion and provide a qualitative description of the transition.

VI. SUMMARY

We have shown in this paper that anharmonicity in the two-dimensional lattice leads us to a nonlinear Hamiltonian system for displacement fields, which exhibits a range of interesting dynamical behavior. For low-energy levels, the dynamics is governed by regular motion about the local minima of the potential surface. As the energy increases, irregular motion becomes more and more pronounced covering an ever increasing area of the phase space. Eventually, at the level corresponding to the central potential maximum the motion is completely chaotic. What is interesting is that increasing the energy further restores regular motion whose amplitude is now larger as it corresponds to oscillations about more than a single potential well. As a physical example, we have discussed the case of surface reconstruction for the tungsten lattice. Although a return to regular motion does not appear to take place, we believe that the approximate nature of the equations of motion invalidates their use above criticality.

ACKNOWLEDGMENTS

This research has been supported by the University of Alberta and by grants from NSERC (Canada). One of the authors (T.A.R.) acknowledges the assistance in numerical computations he received from Dr. M. Kolar and Dr. M. K. Ali from the University of Lethbridge.

[1] C.J. Gorter and T. van Peski-Tinbergen, Physcia **22**, 273 (1956).
[2] G.A. Smolenski, Fiz. Tverd. Tela (Leningrad) **4**, 1095 (1962) [Sov. Phys. Solid State **4**, 807 (1962)].
[3] K.S. Liu and M.E. Fisher, J. Low Temp. Phys. **10**, 655 (1973).
[4] D.S. Webster and M.J.R. Hoch, J. Phys. Chem. Solids **32**, 2663 (1971).
[5] J.C. Toledano and P. Toledano, *The Landau Theory of Phase Transitions* (World Scientific, Singapore, 1987).
[6] Y. Imry, D.J. Scalapino, and L. Gunther, Phys. Rev. B **10**, 2900 (1974).
[7] Y. Ishibashi and V. Dvořák, J. Phys. Soc. Jpn. **44**, 32 (1978).
[8] I. Muševič, B. Žekš, R. Blinc, T. Rasing, and P. Wyder, Phys. Rev. Lett. **48**, 192 (1982).
[9] A. Ribeiro Filho, D.R. Tilley, and B. Žekš, Phys. Lett. A **100**, 247 (1984).
[10] V.G. Makhankov, Phys. Lett. A **81**, 156 (1981).
[11] M. Peyrard, S. Pnevmatikos, and N. Flytzanis, Physica **19D**, 268 (1986).
[12] E. Coquet, M. Peyrard, and H. Büttner, J. Phys. C **21**, 4895 (1988).
[13] A.F. Sadreev, Z. Phys. **73**, 115 (1988).
[14] A. Czachor and B.J.A. Zielińska, Acta. Phys. Pol. A **76**, 631 (1989).
[15] Y.S. Kivshar, Phys. Rev. A **46**, 8652 (1992).
[16] M. K. Ali and R. L. Somorjai, Physica **1D**, 383 (1980).
[17] P. Hawrylak, K.R. Subbaswamy, and S.E. Trullinger, Phys. Rev. D **29**, 1154 (1984).
[18] M.C. Gutzwiller, J. Math. Phys. **112**, 343 (1971).
[19] E.J. Heller, Phys. Rev. Lett. **58**, 1296 (1987).
[20] R.T. Skodje, F. Borondo, and W.P. Reinhardt, J. Chem. Phys. **82**, 4611 (1985).
[21] C.C. Martens, R.L. Waterland, and W.P. Reinhardt, J. Chem. Phys. **90**, 2328 (1989).
[22] N. Deleon and E.J. Heller, J. Chem. Phys. **78**, 4005 (1983).
[23] B. Eckhardt, G. Hose, and E. Pollak, Phys. Rev. A **39**, 3776 (1989).
[24] R.H.G. Helleman and T. Bountis, in *Stochastic Behavior in Classical and Quantum Hamiltonian Systems*, edited by G. Casati and J. Ford, Springer Lecture Notes in Physics Vol. 93 (Springer, Berlin, 1979), p. 353.
[25] M. Founargiotakis, S.C. Frantos, G. Contopoulos, and C. Polymilis, J. Chem. Phys. **91**, 1389 (1989).
[26] T.E. Felter, R.A. Barker, and P.J. Estrup, Phys. Rev. Lett. **38**, 1138 (1977).
[27] R.F. Willis, in *Many-Body Phenomena at Surfaces*, edited by D.C. Langreth and H. Suhl (Academic, New York, 1983).
[28] L.D. Roelofs, G.Y. Hu, and S.C. Ying, Phys. Rev. B **28**, 6369 (1983).
[29] C.L. Fu, A.J. Freeman, E. Wimmer, and M. Weinert, Phys. Rev. Lett. **54**, 2261 (1985).
[30] W.K. Han and S.C. Ying, Phys. Rev. B **41**, 9163 (1990).
[31] J. Kanamori, Ann. Phys. (Paris) **10**, 43 (1985).